Biochemical and Biophysical Research Communications 464 (2015) 459–466

Contents lists available at ScienceDirect

Biochemical and Biophysical Research Communications

journal homepage: www.elsevier.com/locate/ybbrc

Integrin LFA-1 regulates cell adhesion via transient clutch formation

Munenori Ishibashi [a, b, 1], Yukihiro Miyanaga [a, b], Satomi Matsuoka [a, b], Jun Kozuka [a, b], Yuichi Togashi [c], Tatsuo Kinashi [d], Masahiro Ueda [a, b, *]

[a] Laboratory for Cell Signaling Dynamics, QBiC (Quantitative Biology Center), RIKEN, 6-2-3 Furuedai, Suita, Osaka 565-0874, Japan
[b] Department of Biological Sciences, Graduate School of Science, Osaka University, 1-1 Machikaneyama, Toyonaka, Osaka 560-0043, Japan
[c] Research Center for the Mathematics on Chromatin Live Dynamics, Graduate School of Science, Hiroshima University, 1-3-1 Kagamiyama, Higashi-Hiroshima, Hiroshima 739-8526, Japan
[d] Department of Molecular Genetics, Institute of Biomedical Science, Kansai Medical University, 2-5-1 Shin-machi, Hirakata, Osaka 573-1010, Japan

ARTICLE INFO

Article history:
Received 19 June 2015
Accepted 24 June 2015
Available online 2 July 2015

Keywords:
Immune cell
Cell adhesion
Chemokine
Integrin
Single-molecule

ABSTRACT

Integrin LFA-1 regulates immune cell adhesion and trafficking by binding to ICAM-1 upon chemokine stimulation. Integrin-mediated clutch formation between extracellular ICAM-1 and the intracellular actin cytoskeleton is important for cell adhesion. We applied single-molecule tracking analysis to LFA-1 and ICAM-1 in living cells to examine the ligand-binding kinetics and mobility of the molecular clutch under chemokine-induced physiological adhesion and Mn^{2+}-induced tight adhesion. Our results show a transient LFA-1-mediated clutch formation that lasts a few seconds and leads to a transient lower-mobility is sufficient to promote cell adhesion. Stable clutch formation was observed for Mn^{2+}-induced high affinity LFA-1, but was not required for physiological adhesion. We propose that fast cycling of the clutch formation by intermediate-affinity integrin enables dynamic cell adhesion and migration.

1. Introduction

Cell adhesion is important for maintaining tissue integrity and controlling dynamic processes such as immune cell trafficking [1]. Cell adhesion to the extracellular matrix or to each other is mediated by integrins, a family of cell-surface receptors. LFA-1 (leukocyte function-associated antigen 1), also known as $\alpha_L\beta_2$ integrin (CD11a/CD18), is one of the most studied adhesion receptors, and it plays key roles in the trafficking of lymphocytes associated with autoimmune and inflammatory diseases [2] [3], and [4]. Through binding to its ligand ICAM-1 (intercellular adhesion molecule 1, CD54), LFA-1 mediates lymphocyte adhesion to the vessel wall and migration into peripheral lymph nodes. LFA-1-dependent adhesion and migration are regulated by "inside-out signaling" mechanisms involving Rap1 and the actin cytoskeleton [2] and [3]. Rap1, a small G protein activated by chemokine stimulation, is the intracellular activator of LFA-1 for extracellular ICAM-1 binding. The actin cytoskeleton somehow contributes to the maintenance of active LFA-1 for adhesion [5] and [6]. LFA-1-mediated mechanical linkage between extracellular ICAM-1 and the actin cytoskeleton functions as a molecular clutch across the membrane during lymphocyte adhesion and migration [7]. Thus, the dynamics of the molecular clutch is important for understanding how lymphocyte adhesion and migration are regulated.

The relationship between cell adhesion and the ligand-binding stability of the molecular clutch is controversial. According to the most commonly accepted view, when the active state of LFA-1 has a high affinity for ligand binding, it is involved in a stable clutch formation that mediates cell adhesion [5] and [6]. This model is supported by experiments using Mn^{2+} treatment, which is widely used to induce the high affinity form of LFA-1 and strong cell adhesion [8]. On the other hand, other reports have suggested against the stable clutch formation for cell adhesion [9] [10] [11], and [12]. Additionally, one recent study suggested that ICAM-1 binding affinity is low when cells are activated by chemokine stimulation [13]. To reveal the dynamics of the molecular clutch in living cells, single-molecule imaging techniques have been applied to LFA-1 and other integrins [14] [15], and [16]. These single-molecule studies suggested integrin mobility is reduced during

Abbreviations: LFA-1, leukocyte function-associated antigen 1; ICAM-1, intercellular adhesion molecule 1.

* Corresponding author. Laboratory of Single Molecule Biology, Department of Biological Science, Graduate School of Science, Osaka University, 1-1 Machikaneyama, Toyonaka, Osaka 560-0043, Japan.
E-mail address: ueda@bio.sci.osaka-u.ac.jp (M. Ueda).
[1] Present address: Department of Cellular and Molecular Biology, University of Texas Health Science Center at Tyler, USA.

http://dx.doi.org/10.1016/j.bbrc.2015.06.155

cell adhesion, probably due to molecular clutch formation. However, due to a lack of ligand binding measurements, uncertainty remains whether the lowered shift in integrin mobility correlates with ligand binding and whether the high affinity state of integrin is indispensable for physiological adhesion and migration.

In order to reveal the binding kinetics and mobility of LFA-1 during cell adhesion, we applied live-cell single-molecule imaging techniques to both LFA-1 and ICAM-1. A lower LFA-1 mobility for cell adhesion was confirmed as proposed previously, and the amount of low-mobility LFA-1 strongly correlated with the cell adhesive strength. Furthermore, the low-mobility state of LFA-1 was associated with both ICAM-1 and the actin cytoskeleton, thus reflecting the molecular clutch for cell adhesion. Contrary to previous views, stable association between high-affinity LFA-1 and ICAM-1 is not required for chemokine-induced physiological cell adhesion. Instead, a transient formation of the molecular clutch lasting only a few seconds is sufficient to mediate lymphocyte adhesion. Thus, fast cycling of the transient clutch formation may allow lymphocyte adhesion with dynamic migration under physiological conditions.

2. Materials and methods

Detailed methods are available in supplementary information.

2.1. Cell preparation and culture

The α_L and β_2 subunits of human LFA-1 were introduced in non-adherent mouse pro-B-cell line Ba/F3 cells. The wild-type β_2 subunit of human LFA-1 cDNA was inserted into the N terminus of Halo (Promega) to produce LFA-1-Halo. T7-tagged Rap1V12 was introduced further by retrovirus. Expression levels of LFA-1 in the cells were maintained by flow cytometric analysis and cell sorting (Supplementary Fig. S1a, b). The expression of Rap1V12 was confirmed by Western blot analysis (Supplementary Fig. S1c).

2.2. Coating plates with ICAM-1

Glass based dishes (IWAKI) were incubated with anti-Fc antibody at 4 °C overnight and then incubated with recombinant human ICAM-1 Fc chimera (R&D) with and without chemokine SDF-1 (R&D) for 2–4 h at room temperature and then further incubated in PBS containing 1% BSA for 10 min at room temperature.

2.3. Cell adhesion assay

Cells at 0.5×10^5 cells/ml were transferred to ICAM-1- or non-coated plates in the presence or absence of immobilized SDF-1, expressed Rap1V12, or 1 mM of Mn^{2+} with or without 1 μM LatA, and then incubated at 37 °C for 10 min. Non-adherent cells were removed by four consecutive washes, and then input and bound cells were measured using bright-field microscopy.

2.4. Fluorescent labeling of LFA-1 and ICAM-1 molecules

LFA-1-Halo was fluorescently labeled by HaloTag TMR ligand (Promega). Soluble ICAM-1 (R&D) molecules were labeled by NHS-TMR (Thermo).

2.5. TIRF microscopy observation

Single molecule observation of LFA-1 or sICAM-1 molecules in living cells was performed with objective type TIRF microscopy. Cells were observed at 37 °C under TIRF microscopy within 30 min. Non-adherent cells were overlaid with a sheet of 3% agarose and excess medium was removed.

2.6. Single-molecule tracking and statistical analysis

Fluorescent spots, which showed single-step photobleaching (Supplementary Fig. S2a–c), were tracked at video rate (30 frames per sec). The trajectories of individual fluorescent spots were obtained semi-automatically using laboratory-made software. The tracked spots were analyzed further by additional software written in Matlab (Mathworks).

3. Results

3.1. Cell adhesiveness correlates with the amount of low-mobility LFA-1

We previously established a reconstituted system in which mouse pro-B cell line Ba/F3 cells expressing human LFA-1-Halo (α_L/β_2-Halo) can adhere to human ICAM-1 immobilized on glass surfaces in an activation-dependent manner [17] (Supplementary Fig. S1). In order to reveal differences in LFA-1 dynamics between the non-regulated and functional states, the following three cell conditions were analyzed: non-adherent resting cells on uncoated glass (Fig. 1a, None) and two kinds of adherent cells activated by Rap1V12 expression or Mn^{2+} treatment on ICAM-1-coated glass (Fig. 1a, Rap1V12 or Mn^{2+}). The cell adhesive strengths were measured by adhesion assays which showed 0.43%, 54% and 80% of cells were adherent in the three conditions, respectively (Fig. 1b). By combining the reconstitution system with total internal reflection fluorescence (TIRF) microscopy, we successfully visualized single-molecule LFA-1-Halo conjugated with tetramethylrhodamine (TMR) at the adhesive areas of the cells (Fig. 1c and Supplementary Fig. S2a–c). We found that most LFA-1 molecules were mobile and diffused fast on the resting cells. Upon activation of cells with Rap1V12 expression or Mn^{2+} treatment, many LFA-1 molecules were stably immobilized at the adhesive area (Fig. 1d and Supplementary Video 1). The average diffusion coefficient over a 132-ms interval was estimated from the single-molecule trajectories by calculating the mean-square displacement (MSD) [18], which is denoted as $D^{MSD}_{132\ ms}$ hereafter. The histogram of $D^{MSD}_{132\ ms}$ clearly shows two peaks independent of the cellular condition (Fig. 1e), suggesting that LFA-1 adopts at least two diffusion states. The lower-diffusion state increased as the cells became more adhesive, suggesting that it represents the functional state of LFA-1 when interacting with immobilized ICAM-1 (immICAM-1).

Supplementary data related to this article can be found online at http://dx.doi.org/10.1016/j.bbrc.2015.06.155.

To conduct a more quantitative characterizations of the multiple diffusion states, we next estimated the diffusion coefficients based on a distribution of the displacements over a 33-ms interval. The displacement distribution was fitted to a probability density function using maximum likelihood estimation (MLE) and Akaike's information criterion (AIC), as described elsewhere [19] (Fig. 1f and see Methods), to yield an estimation of the minimal model for multiple diffusion states at a temporal resolution of 33 ms. The estimated diffusion coefficient is denoted as $D^{MLE}_{33\ ms}$. The result of this analysis suggested that diffusive movements of LFA-1 molecules could be classified into at least three kinds of mobility: low, middle and high (Fig. 1g and Table 1). The respective diffusion coefficients of the states were 0.025 ± 0.012 (mean ± s.d.) $\mu m^2/s$, 0.13 ± 0.016 $\mu m^2/s$, and 0.37 ± 0.036 $\mu m^2/s$. The threshold for the diffusion coefficient of immobile molecules was 0.046 $\mu m^2/s$ with an accuracy of position of 39 nm in this

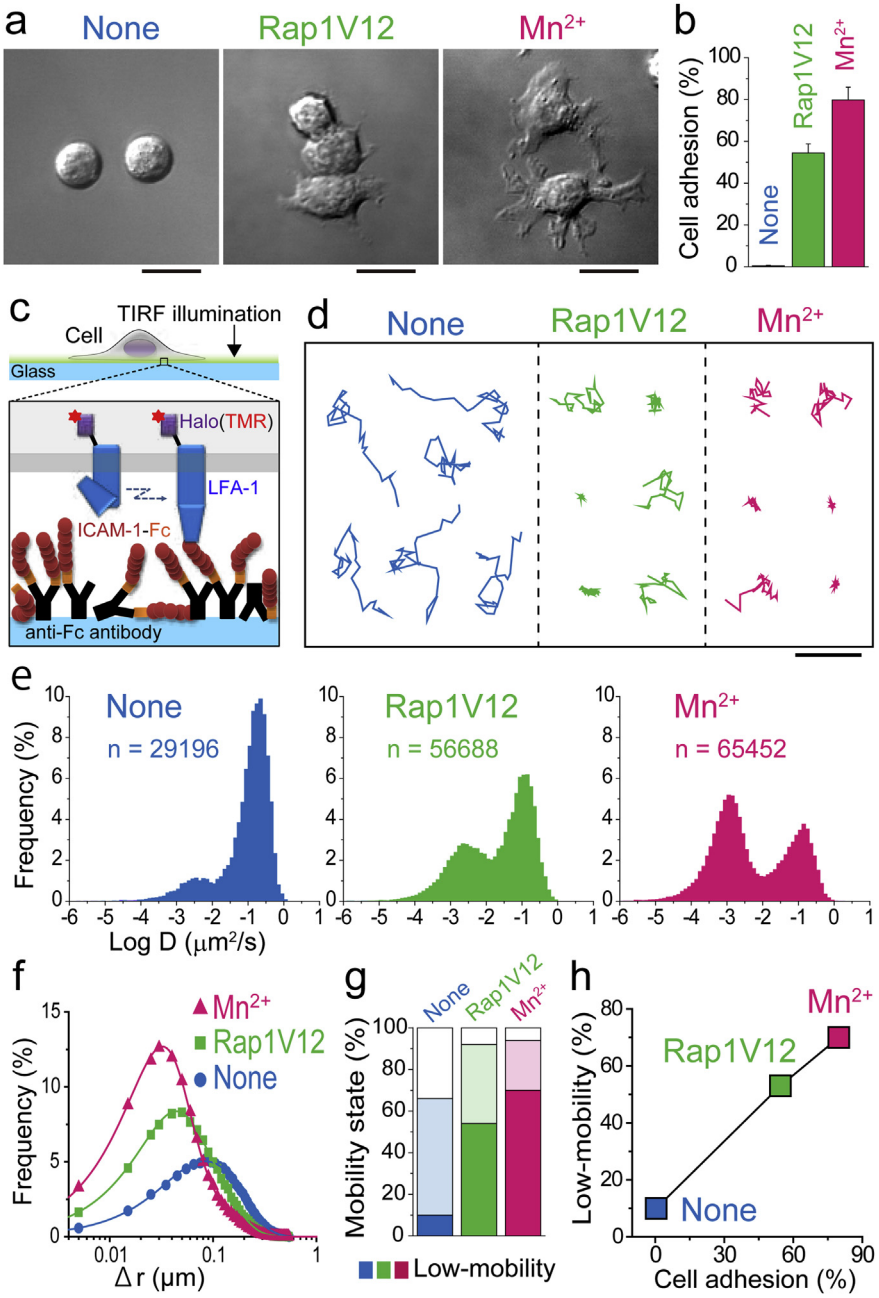

Fig. 1. Low-mobility state of LFA-1 strongly correlated with its adhesive activity. (a) Images of non-adherent resting, Rap1V12 expressed and Mn^{2+} treatmed cells. (b) Cell adhesive strength expressed as a percentage of bound cells after washing out non-adherent cells (mean ± s.e.m.). (c) Scheme of single-molecule imaging of LFA-1-Halo (TMR) at adhesive areas of the cell by TIRF illumination. (d) Typical trajectories of LFA-1 on the membrane over the same 1-s period. (e) Histograms of diffusion coefficients over a time interval of 132 ms calculated by mean square displacement (MSD) plots. (f) The distribution of displacements (Δr) observed in resting, Rap1V12-expressed, and Mn^{2+}-treated cells over a 33-ms period. The fitted curves are lined with the same color of data. (g) Fraction of low- (dark color), middle- (light color), and high- (white) mobility states. (**h**) Correlation between cell adhesiveness and faction of low-mobility LFA-1. Scale bars are 20 μm (a) and 1 μm (d).

analysis (see Methods). Thus, the low-mobility state was assumed immobile. $D_{33\ ms}^{MLE}$ values after correction for errors in the position determination were 0.081 ± 0.012 $\mu m^2/s$ and 0.33 ± 0.016 $\mu m^2/s$ for the middle- and high-mobility states, respectively (see Methods). The high-mobility state could be considered a relatively freely-diffusing state of LFA-1, because its diffusion coefficients were similar to those of lipid molecules on plasma membranes [18]. Diffusion coefficients of the middle-mobility state were similar to typical values of transmembrane proteins [18]. The low-mobility state represents immobile LFA-1, as described above, suggesting that molecules in this state are anchored to immICAM-1 and/or some intracellular structures such as the actin cytoskeleton. The low-mobility state was the major state in Rap1V12-expressed and Mn^{2+}-treated cells, as which 54% and 70% of LFA-1 molecules adopted this state, respectively, while 10% adopted this state in resting cells (Fig. 1g and Table 1). Thus the low-mobility state of LFA-1 became dominant as cells increased their adhesiveness (Fig. 1h), indicating a clear correlation between the amount of low-mobility LFA-1 and the strength of cell adhesion.

3.2. The amount of low-mobility LFA-1 depends on interaction with ICAM-1 and F-actin

To further characterize the low-mobility state of LFA-1 with relevance to its activation and ICAM-1 binding, we examined intracellular effects on LFA-1 mobility by activation in the absence and presence of immICAM-1 (Fig. 2a, b and Table 1). In the absence of ICAM-1, cell adhesion was not induced, and the proportion of the low-mobility states in resting, Rap1V12-expressed and Mn^{2+}-treated cells were 10%, 32% and 26%, respectively. These results showed that LFA-1 activation caused a slight increase in the low-mobility state as a result of anchoring to some intracellular structures such as the actin cytoskeleton. ImmICAM-1 addition further increased the low-mobility state to 15%, 53% and 70%, respectively, showing that interaction between activated LFA-1 and ICAM-1 enhanced the low-mobility state. Cell adhesion was induced when both LFA-1 activation and extracellular ICAM-1 were applied. Taken together, these observations indicate that active LFA-1, which associates with intracellular structures, gives rise to the full increase in the low-mobility state through interaction with the extracellular immICAM-1 and leads to cell adhesion. Thus, the low-mobility state can be regarded as a molecular clutch for cell adhesion.

To examine the contribution of the actin cytoskeleton to cell adhesion or the low-mobility state of active LFA-1, we next analyzed the effect of F-actin disruption on cells stimulated with Rap1V12 expression or Mn^{2+} treatment. Latrunculin A (LatA) of 1 μM successfully decreased submembranous F-actin (Supplementary Fig. S3) and dramatically impaired cell adhesion (Fig. 2a). Consistent with the correlation between cell adhesiveness and the amount of the low-mobility state, F-actin disruption inhibited the low-mobility state of LFA-1 (Fig. 2b, c, Table 1 and Supplementary Video 2). Thus, the actin cytoskeleton is necessary for the low-mobility state of LFA-1 to undergo clutch formation.

Supplementary data related to this article can be found online at http://dx.doi.org/10.1016/j.bbrc.2015.06.155.

The linkage between ICAM-1 and the actin cytoskeleton by LFA-1-mediated molecular clutch was confirmed by imaging single

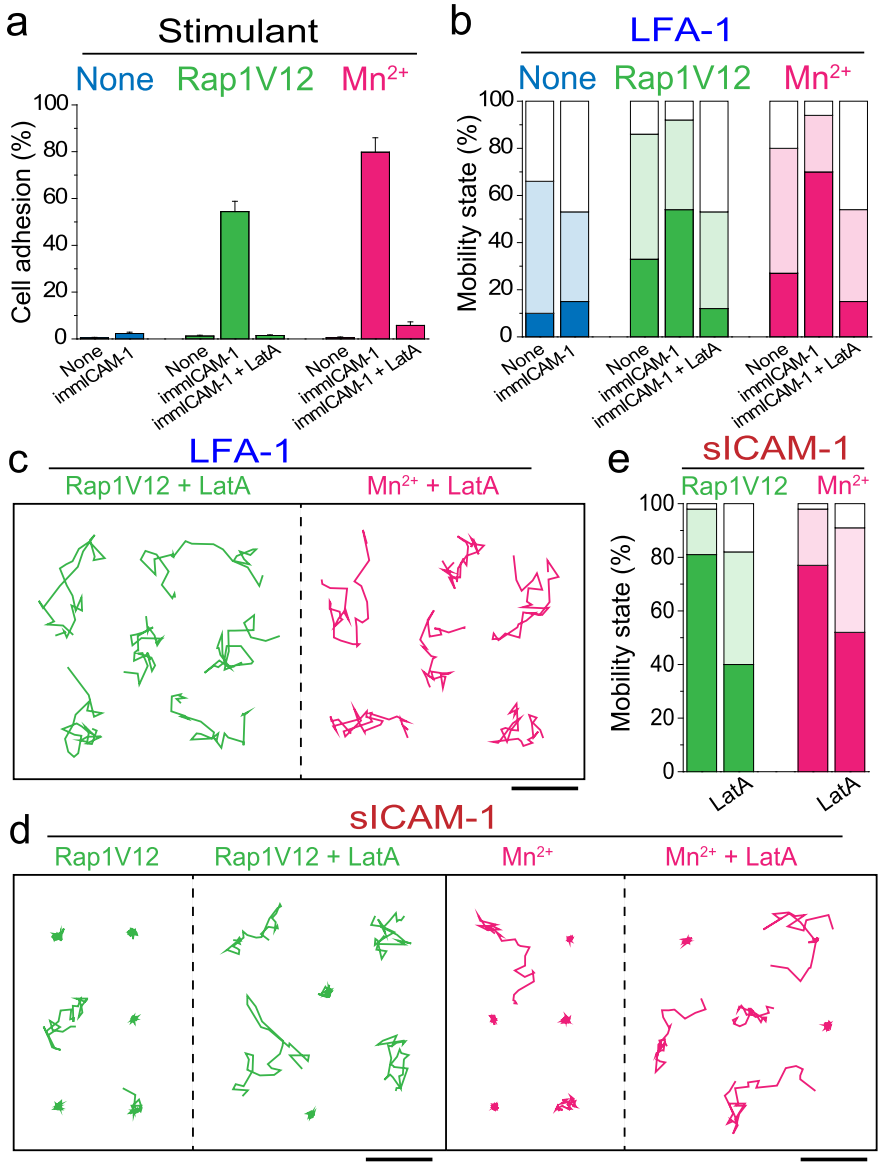

Fig. 2. Low-mobility LFA-1 is associated with both ICAM-1 and F-actin. (**a**) Effects of LFA-1 activation and ICAM-1 binding on cell adhesiveness. (**b**) Effects of LFA-1 activation and ICAM-1 binding on LFA-1 mobility. (**c**) Typical trajectories of LFA-1 in the presence of 1 μM latrunculin A (LatA) for 1 s. (**d**) Typical trajectories of sICAM-1 for 1 s. (**e**) Mobility of soluble ICAM-1 (sICAM-1) bound to cells and effects of F-actin disruption. Scale bars in c, d are 1 μm.

molecules of TMR-labeled soluble ICAM-1 (sICAM-1). sICAM-1 molecules can diffuse freely in the extracellular medium, and their diffusion is restricted only when they bind to LFA-1 on the cells. On cells with Rap1V12 expression or Mn^{2+} treatment, about 80% of sICAM-1 showed the low-mobility state (Fig. 2d, e, Table 2 and Supplementary Video 3). Because sICAM-1 was not immobilized on the glass surface, its low-mobility state indicates an immobilization of its receptor LFA-1 by intracellular structures. F-actin disruption with LatA treatment decreased the proportion of the low-mobility state of sICAM-1 to 40% and 52% in Rap1V12-expressed and Mn^{2+}-treated cells, respectively (Fig. 2d, e and Table 2). This result indicates that LFA-1-mediated clutch formation depends on the interaction with the actin cytoskeleton and ICAM-1.

Supplementary data related to this article can be found online at http://dx.doi.org/10.1016/j.bbrc.2015.06.155.

3.3. Transient binding to ICAM-1 mediates cell adhesion

Single-molecule imaging of sICAM-1 enables us to measure directly the lifetimes of LFA-1/ICAM-1 complexes. Individual fluorescent sICAM-1 spots stochastically appeared on the cell membrane, underwent lateral diffusion and then disappeared from the membrane. The time duration between the appearance and disappearance of the fluorescent spot on the membrane corresponds to an apparent binding duration of sICAM-1 to LFA-1 (Fig. 3a). The histogram of the time durations, which provides the binding probability as a function of time after initiation of the binding, showed an exponential decay under all conditions investigated (Fig. 3b). By fitting the dissociation curves with a sum of two exponential functions after photobleaching calibration, the lifetimes of LFA-1/ICAM-1 complex formation were estimated, and an average lifetime (τ_a) was obtained (Table 3 and see Methods). The two decay times (τ_i) and corresponding proportions in the resting cells were $\tau_1 = 0.085$ s (80%) and $\tau_2 = 1.8$ s (20%), and in Mn^{2+}-treated cells were $\tau_1 = 0.54$ s (59%) and $\tau_2 = 12$ s (41%), from which average lifetimes (τ_a) of the LFA-1/ICAM-1 complex were calculated as 1.5 s and 10 s, respectively. The Mn^{2+}-induced longer lifetime (τ_2) may represent binding to high-affinity LFA-1. To examine whether the contribution from the actin cytoskeleton is required for LFA-1/ICAM-1 complex formation, binding durations were observed for Mn^{2+}-treated cells with F-actin disruption (Fig. 3b and Table 3). The effect of F-actin disruption with LatA was weak against the duration of sICAM-1 binding, even though cell adhesion was dramatically impaired. F-actin disruption with LatA decreased the lifetime of sICAM-1 binding only slightly: $\tau_1 = 0.40$ s (56%), $\tau_2 = 9.1$ s (44%) and average $\tau_a = 8.1$ s (Supplementary Video 3), but reduced the cell adhesive strength from 80% to 5.7%. These results indicate that cell adhesion strongly depends on the intracellular interaction between LFA-1 and the actin cytoskeleton, because cell adhesion was impaired even when stable LFA-1/ICAM-1 binding was maintained. In Rap1V12-expressed cells, the lifetimes of the LFA-1/ICAM-1 complex were $\tau_1 = 0.18$ s (41%), $\tau_2 = 2.0$ s (59%) and $\tau_a = 1.9$ s. Therefore, the Mn^{2+}-induced stable binding was not observed in Rap1V12-expressed cells. On the other hand, the binding state of a few seconds was increased by 39% to mediate cell adhesion. Taken together, the relationships between lifetimes of the LFA-1/ICAM-1 complex and cell adhesiveness (Fig. 3c) indicate that stable ICAM-1 binding with high affinity LFA-1 is not required for cell adhesion, but that the increase in transient clutch formation of a few seconds is.

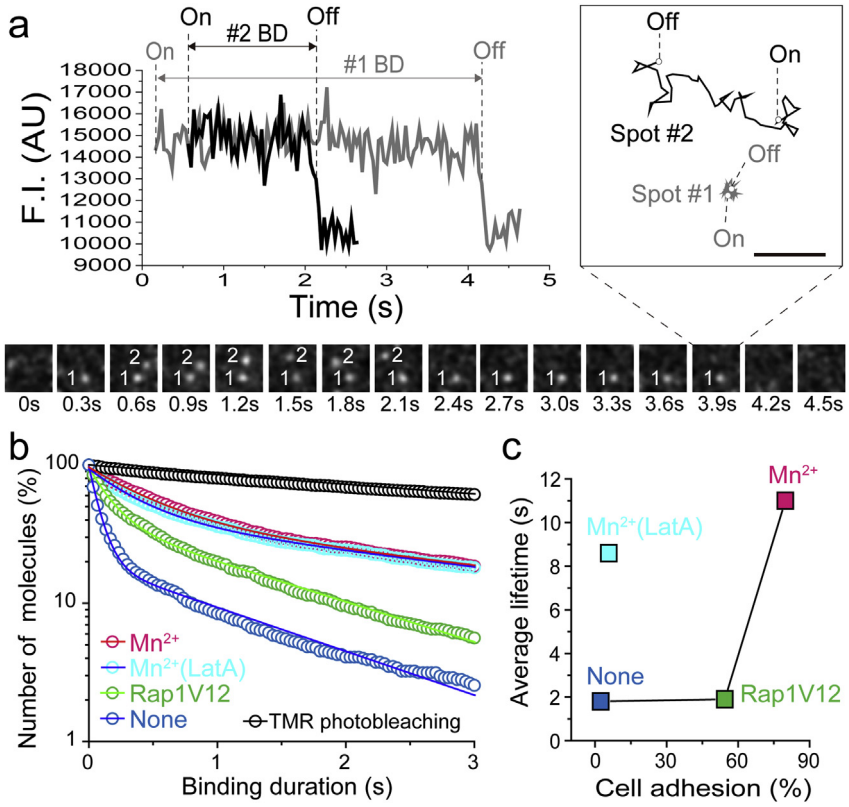

Fig. 3. Transient LFA-1/ICAM-1 interaction mediates cell adhesion. (**a**) Scheme for measurement of apparent binding duration between LFA-1 and ICAM-1. Upper left figure shows time-series of fluorescence intensity (F.I.) of TMR-labeled soluble ICAM-1 bound to a cell. #1 and #2 represent the tracked spots numbered in the time-lapse sequential images below. Apparent binding durations (BD) of each single spot are measured as sustained time of the fluorescent signal from appearance (on) to disappearance (off). Upper right shows trajectories of the tracked spots. Scale bar is 1 μm. (**b**) Dissociation curves of TMR-labeled soluble ICAM-1 bound to cells. Fluorescence decay by photobleaching is also shown for comparison. The fitted curves are overlayed. (**c**) Correlation between cell adhesiveness and corresponding average lifetimes.

3.4. Lymphocyte dynamic adhesion through a transient complex of ICAM-1/LFA-1/F-actin

Chemokine SDF-1 (stromal cell-derived factor 1, CXCL12) activates Rap1 and triggers LFA-1/ICAM-1 interactions, which mediate lymphocyte homing to peripheral lymph nodes, leukocyte recruitment to inflamed tissues, and trafficking of hematopoietic stem cells [2] and [4]. We therefore next examined the effects of SDF-1 to clarify the temporal property of clutch formation by low-mobility LFA-1 under physiological conditions.

Cells stimulated with SDF-1 attached to the glass surface dynamically with migration, while cells firmly attached to the slide when stimulated with Mn^{2+} (Fig. 4a and Supplementary Video 4). This transient attachment explains the low level (13%) of cell

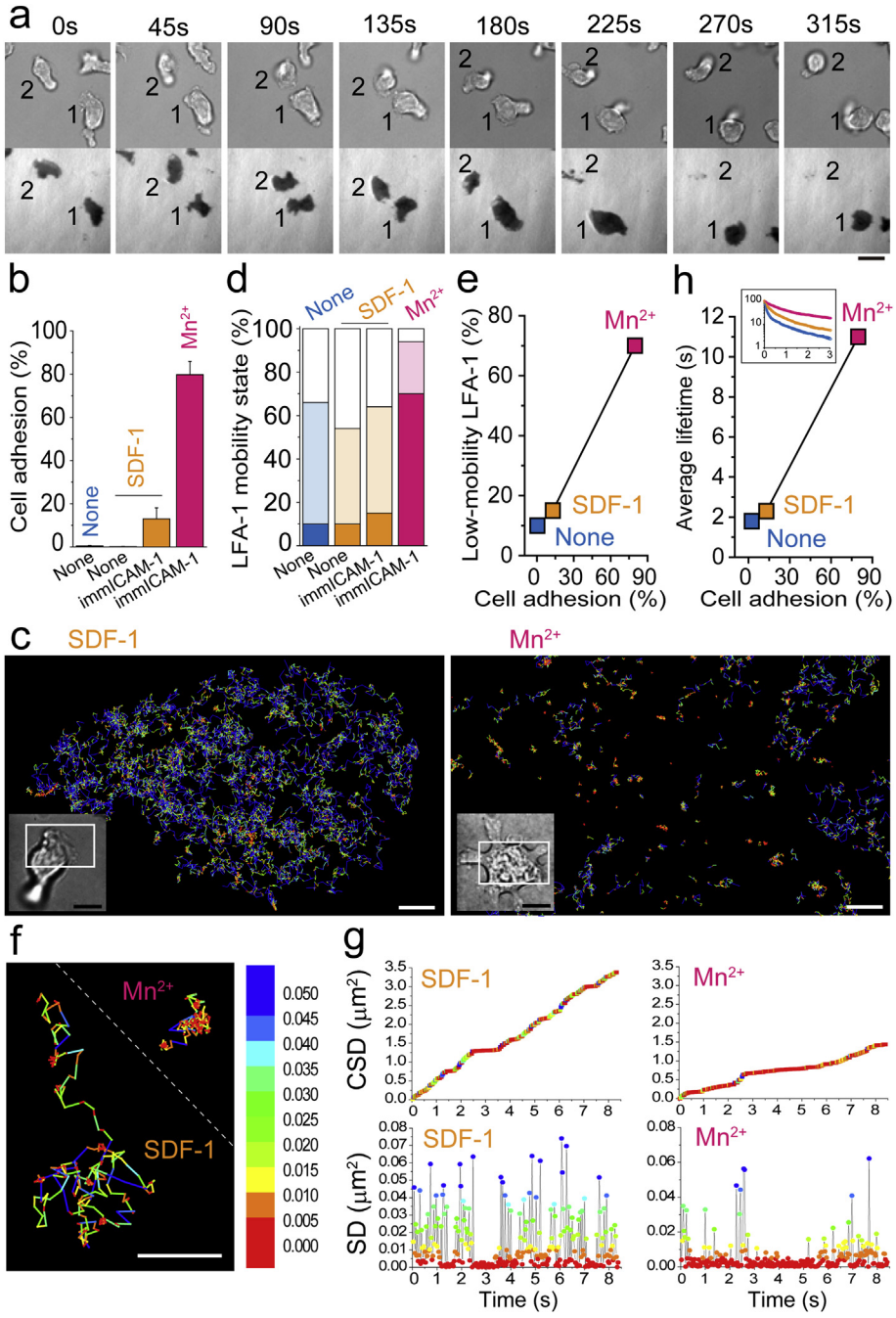

Fig. 4. Chemokine-induced cell adhesion and migration is mediated by transient clutch formation. (**a**) Time-lapse sequential images of cell adhesion and migration. Bright field (top) and interference reflection microscopy (IRM) (bottom). IRM was used to image cell adhesion areas where close contacts became dark areas against bright background. (**b**) Adhesive strength of chemokine-stimulated cells (mean ± s.e.m.). (**c**) Single-molecule trajectories of LFA-1 in SDF-1-stimulated or Mn^{2+}-treated single cell. Bright field images of the cell (insets) were taken before TIRF illumination. Trajectories in the outlined areas of the insets are depicted. The number of data ($n_{\Delta r}$) is 13,588 and 11,603 for SDF-1 and Mn^{2+}, respectively. See Supplementary Fig. S4 for enlarged pictures. (**d**) LFA-1 mobility in chemokine-treated cells. (**e**) Correlation between cell adhesiveness and faction of low-mobility LFA-1. (**f**) Typical trajectories of LFA-1 in chemokine- and Mn^{2+}-treated cells. (**g**) Time-series of squared displacement (SD) and its cumulative values calculated from the trajectories depicted in (f). (**h**) Correlation between cell adhesiveness and corresponding average lifetimes. Inset shows corresponding dissociation curve in which x- and y-axes are binding duration (s) and number of molecules (%), respectively. The same data of non- and Mn^{2+}-stimulation from Figs. 1b, g, h and 3b, c are reproduced in b, d, e, h for comparison. Trajectories and plots of c, f, g are colored by SD values according to the color map in (f). Scale bars are 20 μm (a), 2 μm (c), 10 μm (insets of c) and 1 μm (f).

adhesion (Fig. 4b). Fig. 4c shows a comparable number of LFA-1 trajectories in SDF-1- and Mn^{2+}-stimulated cells to compare mobility (also see Supplementary Fig. S4 and Video 5). LFA-1 molecules were much more mobile and diffused much faster in the SDF-1-stimulated cell than in Mn^{2+}-stimulated cell. $D_{33\ ms}^{MLE}$ analysis showed that in SDF-1-stimulated cells, the low-mobility state of LFA-1 increased by only 5% in an ICAM-1-dependent manner (Fig. 4d and Table 1), and the fraction of low-mobility LFA-1 correlated with cell adhesiveness (Fig. 4e), as described above. To clarify the difference in LFA-1 mobility between SDF-1- and Mn^{2+}-stimulated cells, typical single tracks were analyzed by calculating the squared displacement (SD) at 33 ms intervals and cumulative squared displacement (CSD). The low-mobility state of LFA-1 is represented by the duration with low SD values and decreased slopes in the CSD plot (Fig. 4f,g). Mn^{2+}-induced active LFA-1 showed stable arrest, but SDF-1-activated LFA-1 showed transient arrest. This contrasting property indicates that molecular clutch formation is transient at adhesive areas in chemokine-stimulated cells.

Supplementary data related to this article can be found online at http://dx.doi.org/10.1016/j.bbrc.2015.06.155.

To confirm the transient binding between chemokine-activated LFA-1 and ICAM-1, the lifetime of sICAM-1 binding was measured in SDF-1-stimulated cells. The lifetimes of ICAM-1 binding were $\tau_1 = 0.23$ s (70%), $\tau_2 = 2.7$ s (30%) and $\tau_a = 2.2$ s (Fig. 4h, Table 3 and Supplementary Video 6). Thus, the binding state of a few seconds was increased by 10% to mediate cell adhesion. The correlation between the average lifetime and cell adhesiveness was similar to the correlation between the amount of low-mobility LFA-1 and cell adhesiveness (Fig. 4e,h), indicating that transient ICAM-1 binding for 2.2 s is responsible for the 5% increase of low-mobility LFA-1 in chemokine-activated cells. Cytoskeletal interactions with the ICAM-1/LFA-1 complex were confirmed by $D_{33\ ms}^{MLE}$ analysis of both LFA-1 and sICAM-1. The 5% increase of the low-mobility state of LFA-1 was totally impaired by F-actin disruption (Table 1 and Supplementary Fig. S5a). Most (77%) of the membrane-bound sICAM-1 was in the low-mobility state, which was LatA-sensitive (Table 2 and Supplementary Fig. S5b). F-actin disruption suppressed the 10% increase of the binding state of a few seconds: $\tau_1 = 0.089$ s (81%), $\tau_2 = 1.3$ s (19%) (Table 3). A transient integrin-ligand interaction of a few seconds enables flexible regulation of the molecular clutch, which is thought to be associated with the dynamic control of cell adhesion. This fast and flexible regulation of LFA-1/ICAM-1 interaction *in vivo* would make cellular responses to environmental changes more efficient.

Supplementary data related to this article can be found online at http://dx.doi.org/10.1016/j.bbrc.2015.06.155.

4. Discussion

To clarify the relationship between cell adhesiveness, the lateral mobility of integrin and the integrin-ligand binding property, both LFA-1 and ICAM-1 were visualized at adhesive areas. Our results demonstrated that extracellular stable binding between LFA-1 and ICAM-1 is not required for cell adhesion. Instead, transient mechanical linkage between ligand-bound LFA-1 and the intact actin cytoskeleton is sufficient to mediate lymphocyte adhesion.

Our study provides a new model where cell adhesion is regulated via a transient clutch formation that lasts only a few seconds. It has been widely agreed, however, that high affinity LFA-1 results in stable clutch formation with ICAM-1 to promote cell adhesion. Several studies of LFA-1 structures have provided a basis of the affinity regulation [3]. LFA-1 molecules transition between closed, intermediate and open conformations. When these conformations are stabilized by mutations, the mimetic closed, intermediate and open forms result in low-, intermediate- and high-affinity binding to ICAM-1, respectively [20]. Several experiments combined with Mn^{2+} treatment have suggested stable clutch formation accompanied by high-affinity ligand binding for cell adhesion. Yet the relationship between cell adhesion and the stability of clutch formation is controversial, because no significant increase in ligand binding affinity has been observed even when cell adhesion was promoted [9] [10] [11], and [12]. Thus, the stability of the LFA-1-mediated clutch remains an open question. We therefore visualized not only integrin diffusion but also ligand binding. Our results showed that cell adhesion was mediated by an increase in the amount of low-mobility LFA-1 as a result of molecular clutch formation and that Mn^{2+}-induced integrin clutch was stable, which is consistent with the affinity regulation model. However, our results also revealed that a transient, unstable molecular clutch mediates physiological cell adhesion upon chemokine-stimulation (Supplementary Fig. S6). The lifetime of the clutch formation of a few seconds is consistent with a ligand binding time (2.3 s) of the intermediate form [20]. Taken together, we propose the transient molecular clutch is formed through an intermediate conformation of LFA-1 after activation by chemokine.

Our findings suggest that LFA-1-mediated transient clutch formation is important for dynamic cell adhesion and migration. Chemokine-stimulated cells showed transient LFA-1/ICAM-1 binding of only a few seconds and that only a 5% increase in the low-mobility state of LFA-1 occurred upon interaction with immobilized ICAM-1 via fast transitions. The fast cycling of the molecular clutch formation could be important for controlling lymphocyte dynamics *in vivo* including actions like rolling, arrest, and firm adhesion [11].

Acknowledgments

We thank R. Hamaguchi for technical assistance, Drs. P. Karagiannis and S. Young for critical reading of the manuscript. This work was supported by a Grant-in-Aid from the Ministry of Education, Science, Sports, and Culture of Japan 22111992, and by the Japan Science and Technology Agency, Core Research for Evolutional Science and Technology (CREST).

Appendix A. Supplementary data

Supplementary data related to this article can be found at http://dx.doi.org/10.1016/j.bbrc.2015.06.155.

Transparency document

Transparency document related to this article can be found online at http://dx.doi.org/10.1016/j.bbrc.2015.06.155.

References

[1] R.O. Hynes, Integrins: bidirectional, allosteric signaling machines, Cell 110 (2002) 673–687.
[2] T. Kinashi, Intracellular signalling controlling integrin activation in lymphocytes, Nat. Rev. Immunol. 5 (2005) 546–559.
[3] B.-H. Luo, C.V. Carman, T.A. Springer, Structural basis of integrin regulation and signaling, Annu. Rev. Immunol. 25 (2007) 619–647.
[4] T. Lapidot, A. Dar, O. Kollet, How do stem cells find their way home? Blood 106 (2005) 1901–1910.
[5] N. Hogg, I. Patzak, F. Willenbrock, The insider's guide to leukocyte integrin signalling and function, Nat. Rev. Immunol. 11 (2011) 416–426.
[6] R. Alon, S.W. Feigelson, Chemokine-triggered leukocyte arrest: force-regulated bi-directional integrin activation in quantal adhesive contacts, Curr. Opin. Cell Biol. 24 (2012) 670–676.
[7] M. Vicente-Manzanares, C.K. Choi, A.R. Horwitz, Integrins in cell migration – the actin connection, J. Cell Sci. 122 (2009), 1473–1473.
[8] I. Dransfield, C. Cabañas, A. Craig, N. Hogg, Divalent cation regulation of the function of the leukocyte integrin LFA-1, J. Cell Biol. 116 (1992) 219–226.

[9] M.P. Stewart, C. Cabanas, N. Hogg, T cell adhesion to intercellular adhesion molecule-1 (ICAM-1) is controlled by cell spreading and the activation of integrin LFA-1, J. Immunol. 156 (1996) 1810–1817.
[10] E. Sebzda, M. Bracke, T. Tugal, N. Hogg, D.A. Cantrell, Rap1A positively regulates T cells via integrin activation rather than inhibiting lymphocyte signaling, Nat. Immunol. 3 (2002) 251–258.
[11] A. Salas, M. Shimaoka, A.N. Kogan, C. Harwood, U.H. von Andrian, T.A. Springer, Rolling adhesion through an extended conformation of integrin alpha L beta 2 and relation to alpha I and beta I-like domain interaction, Immunity 20 (2004) 393–406.
[12] Y. van Kooyk, S.J. van Vliet, C.G. Figdor, The actin cytoskeleton regulates LFA-1 ligand binding through avidity rather than affinity changes, J. Biol. Chem. 274 (1999) 26869–26877.
[13] T. Schürpf, T.A. Springer, Regulation of integrin affinity on cell surfaces, EMBO J. 30 (2011) 4712–4727.
[14] C.W. Cairo, R. Mirchev, D.E. Golan, Cytoskeletal regulation couples LFA-1 conformational changes to receptor lateral mobility and clustering, Immunity 25 (2006) 297–308.
[15] G.J. Bakker, C. Eich, J.A. Torreno-Pina, R. Diez-Ahedo, G. Perez-Samper, T.S. van Zanten, et al., Lateral mobility of individual integrin nanoclusters orchestrates the onset for leukocyte adhesion, Proc. Natl. Acad. Sci. U. S. A 109 (2012) 4869–4874.
[16] O. Rossier, V. Octeau, J.-B. Sibarita, C. Leduc, B. Tessier, D. Nair, et al., Integrins β(1) and β(3) exhibit distinct dynamic nanoscale organizations inside focal adhesions, Nat. Cell Biol. 14 (2012) 1057–1067.
[17] K. Katagiri, M. Hattori, N. Minato, S.K. Irie, K. Takatsu, T. Kinashi, Rap1 is a potent activation signal for leukocyte function-associated antigen 1 distinct from protein kinase C and phosphatidylinositol-3-OH kinase, Mol. Cell. Biol. 20 (2000) 1956–1969.
[18] M.J. Saxton, K. Jacobson, Single-particle tracking: applications to membrane dynamics, Annu. Rev. Biophys. Biomol. Struct. 26 (1997) 373–399.
[19] S. Matsuoka, T. Shibata, M. Ueda, Statistical analysis of lateral diffusion and multistate kinetics in single-molecule imaging, Biophys. J. 97 (2009) 1115–1124.
[20] M. Shimaoka, C. Lu, R.T. Palframan, U.H. von Andrian, A. McCormack, J. Takagi, et al., Reversibly locking a protein fold in an active conformation with a disulfide bond: integrin alphaL I domains with high affinity and antagonist activity in vivo, Proc. Natl. Acad. Sci. U. S. A 98 (2001) 6009–6014.